Photoabsorption off nuclei with self-consistent vertex corrections

F. Riek* and M. F. M. Lutz
Gesellschaft für Schwerionenforschung (GSI), Planck Strasse 1, D-64291 Darmstadt, Germany

C. L. Korpa
Department of Theoretical Physics, University of Pecs, Ifjusag u. 6, H-7624 Pecs, Hungary
(Received 26 September 2008; published 7 August 2009)

We study photoproduction off nuclei based on a self-consistent and covariant many-body approach for the pion and isobar propagation in infinite nuclear matter. For the first time the t-channel exchange of an in-medium pion is evaluated in the presence of vertex correction effects consistently. In particular the interference pattern with the s-channel in-medium nucleon and isobar exchange contribution is considered. Electromagnetic gauge invariance is kept as a consequence of various Ward identities obeyed by the computation. Adjusting the set of Migdal parameters to the data set we predict an attractive mass shift for the isobar of about 50 MeV at nuclear saturation density.

DOI: 10.1103/PhysRevC.80.024902 PACS number(s): 25.20.Dc, 24.10.Jv, 21.65.−f, 13.75.Gx

I. INTRODUCTION

There is empirical evidence from photon nucleus absorption cross sections that the delta resonance changes its properties in nuclear matter substantially already at nuclear saturation density [1–3]. The microscopic description of the isobar self-energy is a challenge taken up by various groups [4–16]. Naturally, the study of the latter requires a solid understanding of the pion spectral function in nuclear matter (see, e.g., Refs. [16–19] and references cited in Ref. [16]).

The phenomenological spreading potential [1] suggests a small repulsive mass shift of the isobar together with an increase of its width. Also recent data on electroproduction of isobars off helium-3 appear consistent with the latter interpretation [3]. With the exceptions of Refs. [5,11,14] model computations of the isobar self-energy claim results compatible with a small repulsive mass shift. On naive grounds one may reject the works [5,11,14] that predict a sizable attractive mass shift for the isobar as being unrealistic and incompatible with nuclear photoabsorption data. However, the situation is not clear-cut. First, one may observe that various detailed works [9,12] adjust their model parameters to reproduce the spreading potential [1] and therefore cannot be taken as a microscopic confirmation of a repulsive isobar mass shift. Second, one should recall the argument put forward in Refs. [5,6,11] that the apparent mass shift seen in photoabsorption data is affected significantly by short-range correlation effects. Thus an attractive isobar mass shift cannot be ruled out, since the phenomenological spreading potential [1] is effective in the sense that the latter effects were not explicitly accounted for.

The purpose of this work is a study of the photoabsorption cross section off nuclei based on a self-consistent and covariant many-body approach for the pion and isobar propagation in infinite nuclear matter that takes into account short-range correlation effects consistently. We will apply the pion and isobar propagator as determined in Ref. [16] within a novel covariant approach where vertex effects parametrized by Migdal's parameters are considered self-consistently. Phenomenological soft form factors that would suppress vertex correction effects artificially are avoided in Ref. [16]. Scalar and vector mean fields for the nucleon and isobar are incorporated consistently.

In the isobar region the t-channel pion-exchange process is known to define a sizable background term for the $\gamma\, p \to \pi^+ n$ reaction [4,17]. Thus it is crucial to consider the t-channel exchange of an in-medium pion on equal footing as the in-medium exchange of the isobar when computing the photoabsorption cross section of nuclei. In this work, for the first time, photoabsorption is considered in the presence of short-range correlation effects in the $\gamma\,\pi\,\pi$, $\gamma\, N\,\Delta$, $\gamma\,\pi\, N\,\Delta$, $\pi\, N\,\Delta$, and $\pi\, N\, N$ vertices. Electromagnetic gauge invariance is kept as a consequence of a series of Ward identities obeyed in the computation. In particular, the interference of the in-medium s-channel isobar exchange and the t-channel in-medium pion exchange is considered.

The set of Migdal parameters is adjusted to obtain agreement with nuclear photoabsorption data [2]. As a firm prediction we obtain an attractive mass shift for the isobar of about 50 MeV at nuclear saturation densities. A comprehensive discussion of the relevance of various many-body effects is given.

II. PHOTOABSORPTION CROSS SECTION

We specify the isobar-hole model in its covariant form [16,20,21]. The interaction of pions with nucleons and isobars is modeled by the leading order vertices

$$\mathcal{L}_{\rm int} = \frac{f_N}{m_\pi}\,\bar\psi\,\gamma_5\,\gamma^\mu\,(\partial_\mu\vec\pi\,)\,\vec\tau\,\psi + \frac{f_\Delta}{m_\pi}\,(\bar\psi^\mu(\partial_\mu\vec\pi\,)\,\vec T\,\psi + \text{h.c.})$$
$$+ g'_{11}\frac{f_N^2}{m_\pi^2}\,(\bar\psi\,\gamma_5\,\gamma_\mu\,\vec\tau\,\psi)\,(\bar\psi\,\gamma_5\,\gamma^\mu\,\vec\tau\,\psi)$$
$$+ g'_{22}\frac{f_\Delta^2}{m_\pi^2}\,((\bar\psi_\mu\,\vec T\,\psi)\,(\bar\psi\,\vec T^\dagger\psi^\mu)$$

*Current affiliation: Cyclotron Institute and Physics Department, Texas A&M University, College Station, Texas 77843-3366, USA.

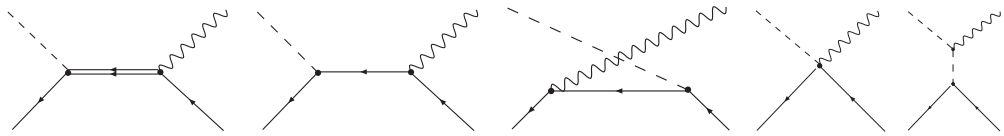

FIG. 1. Feynman diagrams for photon-induced pion production.

$$+((\bar\psi_\mu\,\vec T\,\psi)\,(\bar\psi^\mu\,\vec T\,\psi)+\text{h.c.}))$$
$$+\,g'_{12}\,\frac{f_N\,f_\Delta}{m_\pi^2}\,(\bar\psi\,\gamma_5\,\gamma_\mu\,\vec\tau\,\psi)((\bar\psi^\mu\vec T\,\psi)+\text{h.c.}), \qquad (1)$$

where we use $T_i^\dagger\,T_j=\delta_{ij}-\tau_i\,\tau_j/3$ together with the free-space values $f_N=0.988$ and $f_\Delta=1.85$ in this work. We consider Migdal's short-range correlation vertices as introduced in Refs. [20,21], where it is understood that the local vertices are to be applied at the Hartree level. The Fock contribution can be cast into the form of a Hartree contribution by a simple Fierz transformation. Therefore it only normalizes the coupling strength in Eq. (1) and can be omitted here.

We supplement Eq. (1) by leading order and relevant electromagnetic vertices

$$\begin{aligned}\mathcal{L}_{\text{e.m.}} &= -e\,A^\mu\,\bar\psi\,\frac{1+\tau_3}{2}\,\gamma_\mu\,\psi-e\,A^\mu\,(\vec\pi\times(\partial_\mu\vec\pi))_3\\ &\quad-e\,A_\mu\,\frac{f_N}{m_\pi}\,\bar\psi\,\gamma_5\,\gamma^\mu\,(\vec\tau\times\vec\pi)_3\,\psi\\ &\quad+\frac{i\,f_\gamma}{2\,m_\pi^2}\,(\epsilon_{\mu\nu\alpha\beta}F^{\alpha\beta}\,(\partial^\mu\bar\Psi^\nu)\,T_3\,\psi+\text{h.c.})\\ &\quad+\frac{f'_\gamma}{m_\pi^2}\,(F_{\mu\nu}\,(\partial^\mu\bar\Psi^\nu)\,\gamma_5\,T_3\psi+\text{h.c.}),\end{aligned} \qquad (2)$$

with the electromagnetic field strength tensor $F_{\mu\nu}=\partial_\mu A_\nu-\partial_\mu A_\nu$. The magnetic and electric coupling constants f_γ and f'_γ are determined from the photon-induced pion production cross section off the proton. We compute the cross sections as defined by the diagrams of Fig. 1. The contribution of the u-channel isobar exchange is much suppressed and therefore neglected. The isobar propagator is specified in Ref. [16]. It is modeled by a one-loop self-energy describing the leading decay process of the isobar into a pion and a nucleon. As illustrated in Fig. 2 in the isobar region the photon-proton cross sections are reasonably well described by the electric and magnetic coupling constants $f_\gamma=0.012$ and $f'_\gamma=0.024$. Our values are close to the ones of Pascalutsa and Phillips, $f_\gamma\simeq 0.009$ and $f'_\gamma\simeq 0.021$ [25]. Whereas the neutral pion production is dominated by the s-channel isobar exchange contribution, the production of the charged pion shows a sizable background contribution. Following the arguments put forward in Ref. [16], we consider the Lagrangian densities ((1), (2)) to be effective and allow their parameters to have a residual but smooth density dependence. The latter reflects the dynamics of modes that are integrated out and therefore not treated explicitly here.

We compute the photoabsorption cross section for an "ideal" infinite nucleus. Our studies will be based on the in-medium nucleon propagator parametrized in terms of scalar and vector means fields:

$$\begin{aligned}\mathcal{S}(p) &= \frac{1}{\not p-\Sigma_V^N\not u-m_N+i\,\epsilon}+\Delta S(p),\\ m_N &= m_N^{\text{vac}}-\Sigma_N^S,\\ \Delta S(p) &= 2\,\pi\,i\,\Theta\big[p\cdot u-\Sigma_V^N\big]\,\delta\big[\big(p-\Sigma_V^N\,u\big)^2-m_N^2\big]\\ &\quad\times(\not p-\Sigma_V\not u+m_N)\,\Theta\big[k_F^2+p^2-(u\cdot p)^2\big],\end{aligned} \qquad (3)$$

where the Fermi momentum k_F specifies the nucleon density ρ with

$$\rho=-2\,\text{tr}\,\gamma_0\int\frac{d^4p}{(2\pi)^4}\,i\,\Delta S(p)=\frac{2\,k_F^3}{3\,\pi^2\,\sqrt{1-\vec u^{\,2}/c^2}}. \qquad (4)$$

In the rest frame of the bulk with $u_\mu=(1,\vec 0\,)$ one recovers with Eq. (4) the standard result $\rho=2\,k_F^3/(3\,\pi^2)$. We assume isospin-symmetric nuclear matter. The isobar propagator

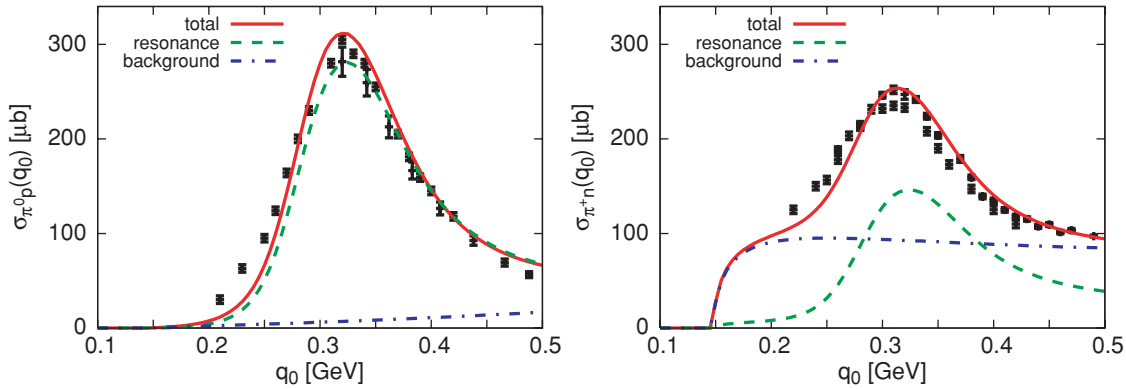

FIG. 2. (Color online) The photoabsorption cross section on the free proton evaluated in terms of the isobar propagator of Ref. [16]. The data points are taken from Refs. [22–24].

$S_{\mu\nu}(w)$ is the solution of Dyson's equation

$$
\begin{aligned}
S_0^{\mu\nu}(w) &= \frac{-1}{\not{w} - m_\Delta + i\,\epsilon} \\
&\quad \times \left(g^{\mu\nu} - \frac{\gamma^\mu\,\gamma^\nu}{3} - \frac{2\,w^\mu\,w^\nu}{3\,m_\Delta^2} - \frac{\gamma^\mu\,w^\nu - w^\mu\,\gamma^\nu}{3\,m_\Delta} \right), \\
S_{\mu\nu}(w) &= S^{(0)}_{\mu\nu}\big(w - \Sigma_V^\Delta\,u\big) \\
&\quad + S^{(0)}_{\mu\alpha}\big(w - \Sigma_V^\Delta\,u\big)\,\Sigma^{\alpha\beta}(w) S_{\beta\nu}(w),
\end{aligned}
\tag{5}
$$

where we allow for scalar and vector mean fields of the isobar with $m_\Delta = m_\Delta^{\rm vac} - \Sigma_S^\Delta$ as developed in Refs. [16,26,27]. In Ref. [16] the pion and isobar self-energy $\Sigma^{\alpha\beta}(w,u)$ were determined in a self-consistent and covariant many-body approach based on the Lagrangian density [Eq. (1)]. In this work we take the results of Ref. [16] and consider the pion and isobar propagators as a function of f_N, f_Δ, and g'_{ij} and the mean-field parameters for the nucleon and isobar. For details on the pion and isobar self-energies we refer to Ref. [16]. It is the aim of the present work to find sets of parameters that lead to a faithful representation of the nuclear photoabsorption data.

The computation of the total absorption cross section is performed in the nuclear matter rest frame. Fermi motion effects are considered. We express the cross section

$$
\begin{aligned}
\sigma_{\gamma A}(q_0) &= \frac{4}{\rho}\int_0^{k_F} \frac{d^3p}{(2\pi)^3}\frac{\Im A_{\gamma N\to\gamma N}(q,p)}{2\,(p - u\,\Sigma_V)\cdot q}, \\
p_0 &= \sqrt{m_N^2 + \vec{p}^{\,2}} + \Sigma_V, \\
q_0 &= |\vec{q}\,|, \qquad u_\mu = (1,\vec{0}),
\end{aligned}
\tag{6}
$$

in terms of the imaginary part of the forward Compton amplitude $A_{\gamma N\to\gamma N}(p,q)$. We explore the role of intermediate πN, NhN, and ΔhN states with

$$
\begin{aligned}
\Im A_{\gamma\,N\to\gamma N}(q,p) &= \Im A^{(\pi)}_{\gamma\,N\to\gamma N}(q,p) + \Im A^{(\rm ph)}_{\gamma\,N\to\gamma N}(q,p) \\
&\quad + \Im A^{(\rm interference)}_{\gamma\,N\to\gamma N}(q,p), \\
\Im A^{(\pi)}_{\gamma\,N\to\gamma N}(q,p) &= \sum_{\lambda,i}{\rm Tr}\int\frac{d^3l}{(2\pi)^3}\,\frac{\Theta[|\vec{l}\,|-k_F]}{16\,E_l}\,\epsilon^\dagger_\mu(q,\lambda) \\
&\quad \times T^{\dagger,i,\mu}_{\gamma\,N\to\pi N}(q,l;w) \\
&\quad \times (\not{l}+M)\,T^{i,\nu}_{\gamma\,N\to\pi\,N}(l,q;w)\,\epsilon_\nu(q,\lambda) \\
&\quad \times (\not{p}+M)\,\rho^{(\pi)}(|w_0-l_0|,\vec{w}-\vec{l}\,)|_{l_0=E_l+\Sigma_V}, \\
\Im A^{(\rm ph)}_{\gamma\,N\to\gamma N}(q,p) &= \sum_{\lambda,i}{\rm Tr}\int\frac{d^3l}{(2\pi)^3}\,\frac{\Theta[|\vec{l}\,|-k_F]}{16\,E_l}\,\epsilon^\dagger_\mu(q,\lambda) \\
&\quad \times T^{\dagger,i,\alpha\mu}_{\gamma\,N\to{\rm ph}N}(q,l;w)\,(\not{l}+M) \\
&\quad \times T^{i,\beta\nu}_{\gamma\,N\to{\rm ph}\,N}(l,q;w)\,\epsilon_\nu(q,\lambda) \\
&\quad \times (\not{p}+M)\,\rho^{(\rm ph)}_{\alpha\beta}(|w_0-l_0|,\vec{w}-\vec{l}\,)|_{l_0=E_l+\Sigma_V},
\end{aligned}
\tag{7}
$$

where "Tr" denotes the trace in Dirac and flavor space. In this work we will neglect the interference term of the pion and particle-hole contributions. The latter probes the product of the pion and particle-hole production amplitudes. Furthermore, $M = m_N - \not{u}\,\Sigma_V$ and $w = p + q$ and $E_l^2 = m_N^2 + \vec{l}^{\,2}$ with $E_l > 0$. We expect the most important contribution in Eqs. (8) to result from the intermediate πN states, where we consider an effective in-medium pion state characterized by its spectral distribution. The effects from the nucleon-hole-nucleon (NhN) and isobar-hole-nucleon (ΔhN) states are described by a tensor spectral distribution. This is possible since we consider only resonant contributions through the isobar s-channel process, for which the production amplitudes as implied by Eq. (1) are degenerate. Because of phase-space considerations the contribution from the NhN states is much larger as compared to the one of the ΔhN states, at least in the isobar region. This implies that this contribution will be roughly proportional to $(g'_{12})^2$ and will become the more important the larger this value becomes.

We begin with a detailed exposition of the pion and particle-hole spectral distributions $\rho_\pi(q)$ and $\rho^{\alpha\beta}_{\rm ph}(q)$ required in Eqs. (8). The central building blocks, in terms of which they are expressed, are the short-range correlation bubbles

$$
\begin{aligned}
\Pi^{(Nh)}_{\mu\nu}(q) &= 2\,\frac{f_N^2}{m_\pi^2}\int\frac{d^4l}{(2\pi)^4}\,i\,{\rm tr}\left(\Delta S(l)\,\gamma_5\,\gamma_\mu\,\frac{1}{\not{l}+\not{q}-M+i\,\epsilon}\right. \\
&\quad \left.\times\,\gamma_5\,\gamma_\nu + \frac{1}{2}\Delta S(l)\,\gamma_5\,\gamma_\mu\,\Delta S(l+q)\,\gamma_5\,\gamma_\nu\right) \\
&\quad + (q_\mu \to -q_\mu), \\
\Pi^{(\Delta h)}_{\mu\nu}(q) &= \frac{4}{3}\,\frac{f_\Delta^2}{m_\pi^2}\int\frac{d^4l}{(2\pi)^4}\,i\,{\rm tr}\;\Delta S(l) S_{\mu\nu}(l+q) \\
&\quad + (q_\mu \to -q_\mu), \\
\Pi_{\mu\nu}(\bar{q}) &= \begin{pmatrix} \Pi^{(Nh)}_{\mu\nu}(\bar{q}) & 0 \\ 0 & \Pi^{(\Delta h)}_{\mu\nu}(\bar{q}) \end{pmatrix},
\end{aligned}
\tag{8}
$$

where "tr" denotes the trace in Dirac space. Note that the isobar-hole loop function in Eqs. (9) is given in terms of the in-medium isobar propagator as specified in Eq. (6) by the isobar self-energy. Details on the evaluation of the loop tensors [Eqs. (9)] can be found in Ref. [16]. For the spectral distributions $\rho_\pi(q)$ and $\rho^{\alpha\beta}_{\rm ph}(q)$ of Eqs. (8) we find

$$
\begin{aligned}
\Pi_\pi(q) &= -4\,\pi\left(1 + \frac{m_\pi}{m_N}\right) b_{\rm eff}\,\rho - \sum_{i,j=1}^{2} q_\mu \left(\Pi^{\mu\nu}_{ij}(q)\right. \\
&\quad \left. + [\Pi(q)\cdot\chi(q)\cdot\Pi(q)]^{\mu\nu}_{ij}\right) q_\nu, \\
g'_{\mu\nu} &= \begin{pmatrix} g'_{11} & g'_{12} \\ g'_{21} & g'_{22} \end{pmatrix} g_{\mu\nu}, \\
\chi^{\mu\nu}_{ij}(q) &= [(1 - g'\cdot\Pi(q))^{-1}\cdot g']^{\mu\nu}_{ij}, \\
\rho_\pi(q) &= -\Im\frac{1}{q^2 - m_\pi^2 - \Pi_\pi(q)}, \\
\rho^{\alpha\beta}_{\rm ph}(q) &= \Im\chi^{\alpha\beta}_{22}(q),
\end{aligned}
\tag{9}
$$

where we recall the value $b_{\rm eff} \simeq -0.01$ fm from Ref. [16]. The latter value is needed to achieve consistency with the low-density limit, where the pion self-energy is determined by the s-wave pion-nucleon scattering length at $q_\mu = (m_\pi, 0)$.

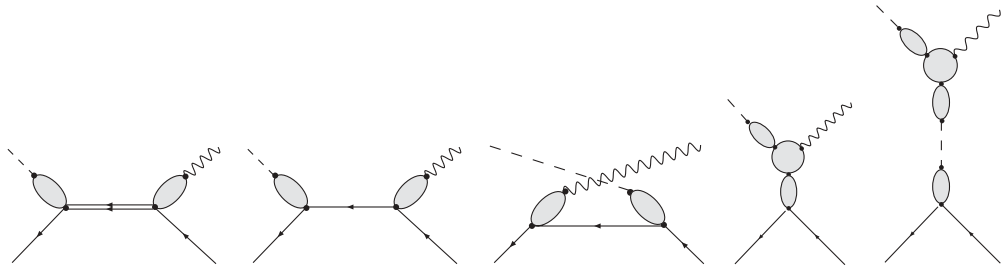

FIG. 3. Feynman diagrams considered for the in-medium $\gamma\, N \to \pi\, N$ process.

We continue with the specification of the pion and particle-hole production amplitudes $T^{i,\mu}_{\gamma\, N\to\pi\, N}$ and $T^{i,\alpha\mu}_{\gamma\, N\to \mathrm{ph}\, N}$ in Eqs. (8). The in-medium generalization of the diagrams of Fig. 1 are shown Fig. 3, where short-range correlation effects are considered in terms of various vertex functions. A similar graphical representation holds for the particle-hole production amplitude, for which, however, we consider resonant contributions only. More explicitly, the in-medium $\gamma\, N \to \pi\, N$ and $\gamma\, N \to \mathrm{ph}\, N$ amplitudes to be used in Eqs. (8) take the form

$$\begin{aligned} T^{\gamma\, N\to\pi N}_{i,\mu}(\bar q, q; w) &= \Lambda^{(\pi N\Delta)}_{i,\,\alpha}(\bar q)\, S^{\alpha\beta}(p+q)\, \Lambda^{(\gamma N\Delta)}_{\mu\beta}(p,q) \\ &\quad + \Lambda^{(\pi NN)}_{i}(\bar q)\, S(p+q)\, \Lambda^{(\gamma\, NN)}_{\mu}(q) \\ &\quad + \Lambda^{(\gamma\, NN)}_{\mu}(q)\, S(\bar p - q)\, \Lambda^{(\pi\, NN)}_{i}(\bar q) \\ &\quad + \Lambda^{(\gamma\,\pi\, NN)}_{i,\mu}(\bar q, q) \\ &\quad + \big[\Lambda^{(\pi NN)}_{i}(\bar q - q),\ \tfrac{1}{2}\tau_3\big]_- S_\pi(\bar q - q) \\ &\quad \times \Lambda^{(\gamma\,\pi\,\pi)}_{\mu}(\bar q, \bar q - q), \\ T^{\gamma\, N\to \mathrm{ph} N}_{i,\alpha\mu}(\bar q, q; w) &= \frac{f_\Delta}{m_\pi}\, T_i^\dagger\, g_{\nu\alpha}\, S^{\nu\beta}(p+q) \Lambda^{(\gamma N\Delta)}_{\mu\beta}(p,q), \end{aligned} \tag{10}$$

where the various vertex functions are subject to the Ward identities

$$\begin{aligned} q^\mu\, \Lambda^{(\gamma\, NN)}_{\mu}(q) &= e\, \frac{1+\tau_3}{2}\, \not q, \quad q^\mu\, \Lambda^{(\gamma\, N\Delta)}_{\mu\nu}(p,q) = 0, \\ (\bar q - q)^\mu\, \Lambda^{(\gamma\,\pi\,\pi)}_{\mu}(\bar q, q) &= e\,(\bar q^2 - q^2 - \Pi_\pi(\bar q) + \Pi_\pi(q)), \\ q^\mu\, \Lambda^{(\gamma\,\pi\, NN)}_{i,\mu}(\bar q, q) &= e\,\big[\tfrac{1}{2}\,\tau_3,\ \Lambda^{\pi NN}_i(\bar q)\big]_- \\ &\quad - e\,\big[\tfrac{1}{2}\,\tau_3,\ \Lambda^{\pi NN}_i(\bar q - q)\big]_-, \end{aligned} \tag{11}$$

with the pion self-energy $\Pi_\pi(q)$ of Eqs. (9). Electromagnetic gauge invariance of the in-medium $\gamma\, N \to \pi\, N$ amplitude [Eqs. (11)] is a consequence of the identities listed in Eqs. (12). The vertex functions of Eqs. (11) take the form

$$\begin{aligned} \Lambda^{(\pi NN)}_{i}(\bar q) &= \frac{f_N}{m_\pi}\, \tau_i\, \bar q_\mu \big(g^{\mu\nu} + [\Pi(\bar q)\cdot\chi(\bar q)]^{\mu\nu}_{11} \\ &\quad + [\Pi(\bar q)\cdot\chi(\bar q)]^{\mu\nu}_{12}\big)\, \gamma_5\gamma_\nu, \\ \Lambda^{(\pi N\Delta)}_{i,\alpha}(\bar q) &= \frac{f_\Delta}{m_\pi}\, T_i^\dagger\, \bar q_\mu\, \big(g^{\mu\nu} + [\Pi(\bar q)\cdot\chi(\bar q)]^{\mu\nu}_{22} \\ &\quad + [\Pi(\bar q)\cdot\chi(\bar q)]^{\mu\nu}_{21}\big)\, g_{\alpha\nu}, \\ \Lambda^{(\gamma\, NN)}_{\mu}(q) &= e\, \frac{1+\tau_3}{2}\, \gamma_\mu, \end{aligned}$$

$$\begin{aligned} \Lambda^{(\gamma\, N\Delta)}_{\mu\alpha}(p,q) &= \frac{i\, f_\gamma}{m_\pi^2}\, T_3\, q^\tau\, \epsilon_{\mu\sigma\tau}{}^\beta \\ &\quad \times \big(g^\sigma_\alpha\, p_\beta + g_{\alpha\rho}\, \chi^{\rho\kappa}_{22}(q)\, \Pi^{(\Delta h)}_{\kappa\sigma,\beta}(q)\big) \\ &\quad - \frac{f'_\gamma}{m_\pi^2}\, T_3\, \gamma_5 (g_{\mu\alpha}\,(p\cdot q) - p_\mu\, q_\alpha), \\ \Lambda^{(\gamma\,\pi\,\pi)}_{\mu}(\bar q, q) &= e\,\Bigg(q_\mu + \bar q_\mu + \sum_{ij=1}^{2}\big([\Pi(q) \\ &\quad + \Pi(q)\cdot\chi(q)\cdot\Pi(q)]^{\nu\beta}_{ij}\, q_\beta + \bar q_\alpha [\Pi(\bar q) \\ &\quad + \Pi(\bar q)\cdot\chi(\bar q)\cdot\Pi(\bar q)]^{\alpha\nu}_{ij}\big)\, g_{\mu\nu} \\ &\quad - \sum_{ijkl=1}^{2} \bar q_\alpha\, [1 + \Pi(\bar q)\cdot\chi(\bar q)]^{\alpha\sigma}_{ik} \\ &\quad \times \Pi^{(kl)}_{\mu,\sigma\tau}(\bar q, q)[1 + \chi(q)\cdot\Pi(q)]^{\tau\beta}_{lj}\, q_\beta\Bigg), \\ \Lambda^{(\gamma\,\pi\, NN)}_{i,\mu}(\bar q, q) &= \frac{e\, f_N}{2\, m_\pi}\, [\tau_3,\ \tau_i]_-\, \gamma_5\, \gamma_\nu \Bigg(\sum_{n=1}^{2}[1 + \Pi(\bar q - q)\cdot \\ &\quad \times \chi(\bar q - q)]^{\beta\nu}_{1n}\, g_{\mu\beta} \\ &\quad - \sum_{jkl=1}^{2} \bar q_\alpha\, [1 + \Pi(\bar q)\cdot\chi(\bar q)]^{\alpha\sigma}_{1k} \\ &\quad \times \Pi^{(kl)}_{\mu,\sigma\tau}(\bar q, \bar q - q)\chi^{\tau\nu}_{lj}(\bar q - q)\Bigg), \end{aligned} \tag{12}$$

with the loop tensors

$$\begin{aligned} \Pi^{(\Delta h)}_{\mu\nu,\alpha}(q) &= \frac{4}{3}\, \frac{f_\Delta^2}{m_\pi^2} \int \frac{d^4 l}{(2\pi)^4}\, i\ \mathrm{tr}\ \Delta S(l) S_{\mu\nu}(l+q)\,(l+q)_\alpha \\ &\quad + (q_\mu \to -q_\mu), \\ \Pi^{(11)}_{\mu,\alpha\beta}(\bar q, q) &= 2\, \frac{f_N^2}{m_\pi^2} \int \frac{d^4 l}{(2\pi)^4}\, i\ \mathrm{tr}\Bigg\{\gamma_5\, \gamma_\beta\, \Delta S(l)\, \gamma_5\, \gamma_\alpha \\ &\quad \times \Bigg[\Bigg(\frac{1}{\not l + \not{\bar q} - M + i\,\epsilon} + \frac{1}{2}\, \Delta S(l + \bar q)\Bigg) \\ &\quad \times \Gamma^{(\gamma\, N\, N)}_{\mu}(l + \bar q, l + q) \\ &\quad \times \Bigg(\frac{1}{\not l + \not q - M + i\,\epsilon} + \frac{1}{2}\, \Delta S(l + q)\Bigg) \end{aligned}$$

$$+\frac{3}{4}\,\Delta S(l+\bar{q})\,\Gamma_{\mu}^{(\gamma\,N\,N)}(l+\bar{q},l+q)\times\Delta S(l+q)\Big]\Big\}-(\bar{q}_\mu,q_\mu)\;\to\;-(\bar{q}_\mu,q_\mu),$$

$$\Pi^{(22)}_{\mu,\alpha\beta}(\bar{q},q)=\frac{4}{3}\,\frac{f_\Delta^2}{m_\pi^2}\int\frac{d^4l}{(2\pi)^4}\,i\,\mathrm{tr}\left\{\Delta S(l)\,S^{\kappa\sigma}(l+\bar{q})\,g_{\alpha\kappa}\times\Gamma^{(\gamma\,\Delta\Delta)}_{\mu,\sigma\tau}(l+\bar{q},l+q)\,S^{\tau\rho}(l+q)\,g_{\beta\rho}\right\}-(\bar{q}_\mu,q_\mu)\;\to\;-(\bar{q}_\mu,q_\mu),$$

$$\Pi^{(12)}_{\mu,\alpha\beta}(\bar{q},q)=\frac{4}{3}\,\frac{f_\gamma}{e\,m_\pi^2}\,\frac{f_N\,f_\Delta}{m_\pi^2}\int\frac{d^4l}{(2\pi)^4}\,i\times\mathrm{tr}\Big\{\gamma_5\,\gamma_\beta\,\Delta S(l)\,S^{\kappa\tau}(l+\bar{q})\,g_{\alpha\kappa}\times\Gamma^{(\gamma\,N\Delta)}_{\mu,\tau}(l+\bar{q},l+q)\times\left(\frac{1}{\not{l}+\not{q}-M+i\,\epsilon}+\Delta S(l+q)\right)\Big\}-(\bar{q}_\mu,q_\mu)\;\to\;-(\bar{q}_\mu,q_\mu).\tag{13}$$

Given the vertices [Eqs. (12)] the Ward identities [Eqs. (12)] follow if the loop tensors $\Pi_{ij}^{\mu,\alpha\beta}(\bar{q},q)$ obey the reduced Ward identities

$$(\bar{q}-q)_\mu\,\Pi_{ij}^{\mu,\alpha\beta}(\bar{q},q)=\delta_{ij}\Pi_{ii}^{\alpha\beta}(q)-\delta_{ij}\,\Pi_{ii}^{\alpha\beta}(\bar{q}).\tag{14}$$

The identities [Eq. (14)] hold provided that the $\gamma\,N\,N$, $\gamma\,N\,\Delta$, and $\gamma\,\Delta\Delta$ vertices in Eqs. (13) satisfy the constraint equations

$$\begin{aligned}&(\bar{p}-p)^\mu\,\Gamma_\mu^{(\gamma\,N\,N)}(\bar{p},p)=\not{\bar{p}}-\not{p},\\&(\bar{p}-p)^\mu\,\Gamma_\mu^{(\gamma\,N\,\Delta)}(\bar{p},p)=0,\\&(\bar{p}-p)^\mu\,\Gamma^{(\gamma\,\Delta\Delta)}_{\mu,\alpha\beta}(\bar{p},p)=[S^{-1}]_{\alpha\beta}(\bar{p})-[S^{-1}]_{\alpha\beta}(p).\end{aligned}\tag{15}$$

We point out that the evaluation of $\Pi_{22}(\bar{q},q)$ required the evaluation of the diagrams of Fig. 3, where the photon couples to the intermediate pion-nucleon state building up the isobar self-energy. This leads to a self-consistency issue, since the latter requires knowledge of the $\gamma\,\pi\,\pi$ vertex, which in turn depends on $\Pi_{22}(\bar{q},q)$.

To make progress we consider the following decomposition:

$$\Pi_{ij}^{\mu,\alpha\beta}(\bar{q},q)=\frac{u_\mu}{u\cdot(\bar{q}-q)}\,\delta_{ij}\left(\Pi_{ii}^{\alpha\beta}(q)-\Pi_{ii}^{\alpha\beta}(\bar{q})\right)+\Delta\Pi_{ij}^{\mu,\alpha\beta}(\bar{q},q),\tag{16}$$

$$(\bar{q}-q)_\mu\,\Delta\Pi_{ij}^{\mu,\alpha\beta}(\bar{q},q)=0,$$

where we argue that the terms $\Delta\Pi_{ij}^{\mu,\alpha\beta}(\bar{q},q)$ are suppressed by $1/m_N$ or $1/m_\Delta$ as compared to the first term in the first of Eqs. (17). This is easily seen for the "11" term. The $\gamma\,N\,N$ vertex takes the form

$$\Gamma_\mu^{(\gamma\,N\,N)}(\bar{p},p)=\gamma_\mu+\frac{2\,i\,f_\gamma}{e\,m_\pi^2}\,\gamma_5\,\gamma_\nu\,\epsilon^{\mu\tau\alpha\beta}\,\chi_{12}^{\nu\kappa}(\bar{p}-p)\times\Pi^{(\Delta h)}_{\kappa\tau,\beta}(\bar{p}-p)\,(\bar{p}-p)_\alpha=\gamma_\mu,\tag{17}$$

where the vertex corrections vanish owing to the antisymmetry of the ε tensor. A further possible contribution proportional to f'_γ is obsolete also. As a consequence $\Delta\Pi_{11}^{\mu,\alpha\beta}(\bar{q},q)$ has a representation, which follows from the one of $\Pi_{11}^{\mu,\alpha\beta}(\bar{q},q)$ in Eqs. (13), upon the replacement

$$\Gamma_\mu^{(\gamma\,N\,N)}=\gamma_\mu\to\gamma_\mu-u_\mu\,\frac{\not{\bar{q}}-\not{q}}{u\cdot(\bar{q}-q)}.\tag{18}$$

The $\gamma\,N\,N$ vertex in Eqs. (13) is sandwiched between two nucleon propagators that are on-shell in the limit of a large nucleon mass. Since vector currents of massive particles are dominated by their zero component, our claim follows. By analogy to the nucleon case, we expect the term $\Delta\Pi_{22}(\bar{q},q)$ to be suppressed by $1/m_\Delta$ as compared to the first term in the first of Eqs. (17). Finally, an explicit analysis of the term $\Delta\Pi_{12}(\bar{q},q)$ reveals also its suppression by $1/m_N$. The $\gamma\,N\,\Delta$ vertex in Eqs. (13) reads

$$\Gamma^{(\gamma\,N\,\Delta)}_{\mu\alpha}(\bar{p},p)=i\,(\bar{p}-p)^\tau\,\epsilon_{\mu\sigma\tau}{}^{\beta}\times\left(g_\alpha^\sigma\,p_\beta+g_{\alpha\rho}\,\chi_{22}^{\rho\kappa}(\bar{p}-p)\,\Pi^{(\Delta h)}_{\kappa\sigma,\beta}(\bar{p}-p)\right)-\frac{f'_\gamma}{f_\gamma}\,\gamma_5(g_{\mu\alpha}\,(p\cdot(\bar{p}-p))-p_\mu\,(\bar{p}-p)_\alpha),\tag{19}$$

where vertex corrections proportional to f'_γ vanish identically. The suppression of $\Delta\Pi_{12}(\bar{q},q)$ follows upon an evaluation of the appropriate trace in Eqs. (13). Thus, in the following we neglect the terms $\Delta\Pi_{ij}^{\mu,\alpha\beta}(\bar{q},q)$ for $i,j=1,2$. It is stressed that the term $u\cdot(\bar{q}-q)$ in Eqs. (17) does not cause any kinematical singularity for on-shell photons with $(\bar{q}-q)^2=0$.

III. NUMERICAL RESULTS AND DISCUSSION

We adjust the set of parameters to the photoabsorption data [2]. For the scalar and vector nucleon mean field we use the values $\Sigma_S^N=0.35$ GeV and $\Sigma_V^N=0.29$ GeV at nuclear saturation density with $k_F=0.27$ GeV as assumed also in Ref. [27]. Following previous works [5,10] an averaged density of 0.8 times saturation density is taken to compute the absorption cross section. We acknowledge an uncertainty implied by the use of an average density instead of folding over a realistic density distribution. However, this approximation is justified for a first determination of the relevant parameter region. The mean-field parameters for the nucleon are extrapolated down to that effective density by a linear ansatz. We obtain a good description of the data [2] when using the following parameter set:

$$\begin{aligned}&\Sigma_S^\Delta=-0.25\ \text{GeV},\qquad\Sigma_V^\Delta=-0.11\ \text{GeV},\\&g'_{11}=1.0,\quad g'_{12}=0.4,\quad g'_{22}=0.4.\end{aligned}\tag{20}$$

An extensive scan in the parameter space was performed. We ensure that given our values for the nucleon mean fields there is a well-defined and localized region in parameter space that leads to an accurate reproduction of the photoabsorption data. A compilation of the results can be found in Figs. 4 and 5. As can be seen from the figures we are only able to determine a certain parameter region. A more precise determination of the parameter set would need a study of more observable processes.

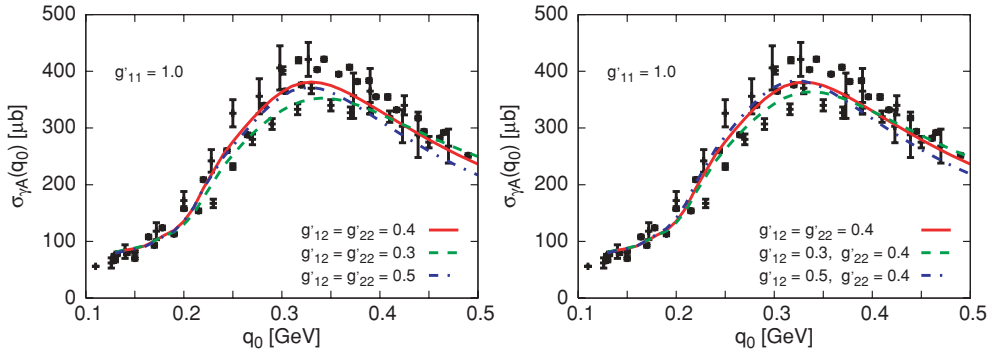

FIG. 4. (Color online) Photoabsorption cross section for variations of g'_{12} and g'_{22}. We always keep $\Sigma_S^\Delta = -0.2$ GeV and $g'_{11} = 1.0$. The following values for Σ_V^Δ are used (corresponding to the legend from top to bottom): -0.09, -0.10, and -0.07 GeV (left panel); -0.09, -0.10, and -0.08 GeV (right panel). All parameters are for 0.8 times saturation density. The data are taken from Ref. [2].

We obtain best agreement with the considered data when using the bare isobar mean fields of Eqs. (20) with opposite sign as compared with the nucleon mean fields. This reflects the distinct treatment of the nucleon and isobar self-energies. Whereas for the nucleon mean-field effects are considered only, the isobar is dressed in addition by complicated loop effects. Thus the bare parameters [Eqs. (20)] do not characterize the physical mass shift of the isobar.

As it turns out we need a reduction of f_Δ and an increase of f_γ as compared to their free-space values. Extrapolating linearly up to nuclear saturation density we derive a 15% reduction of f_Δ and a 15% increase for f_γ. Attempts to describe the data with no in-medium modifications of those parameters fail as the isobar turns too broad and consequently the cross section too small. A reproduction of the data set is possible also by assuming a moderate reduction of f_N. However, this would require an even stronger medium modification of the parameters f_Δ and f_γ. Changes in f'_γ have only a tiny influence on the results so we keep this parameter at its free-space value.

In Fig. 4 we study possible variations of the Migdal parameters g'_{12} and g'_{22} around the central values 0.4 of Eqs. (20). The magnitudes of the Migdal parameters are dependent to some extent on the subtleties of the chosen approach. Thus we refrain from a detailed comparison with values obtained in different schemes. Keeping $g'_{11} = 1.0$ and a scalar mean field for the isobar at $\Sigma_S^\Delta = -0.2$ GeV, we readjust the magnitude for the vector isobar mean field. If we allow for variations larger than 0.1 in the Migdal parameters the cross section can no longer be reproduced accurately. From Fig. 4 we see that with increasing values of g'_{12} and g'_{22} the shape of the cross section gets narrower. The best description is obtained with a parameter set that delivers also the largest overall magnitude for the cross section. Altogether we arrive at values of g'_{12} and g'_{22} of about 0.4. In Fig. 5 we illustrate the effect of lowering Migdal's parameter g'_{11} to 0.6. As seen in the figure such a low value of g'_{11} leads to a significant overshoot of the cross section at small photon energies. Though the resonance contribution itself is not affected much, the background contribution is strongly enhanced. This is shown by the dashed-dotted line, which gives the result implied by all but the first diagram of Fig. 3. We checked that variations of g'_{12}, g'_{22}, or the isobar mean-field parameters do not lead to a significant suppression of this contribution. The only mechanism to arrive at a smaller g'_{11} would be a significant reduction of f_N, however at the price of an even larger reduction of f_Δ. Thus we arrive at a rather large value for $g'_{11} \simeq 1.0$. However, we have to state an uncertainty implied by the neglect of some additional crossed diagrams considered for instance in Ref. [6]. To consolidate the large value for g'_{11} of our study it remains to demonstrate that the inclusion of crossed diagrams does not lower the cross section via subtle interference effects.

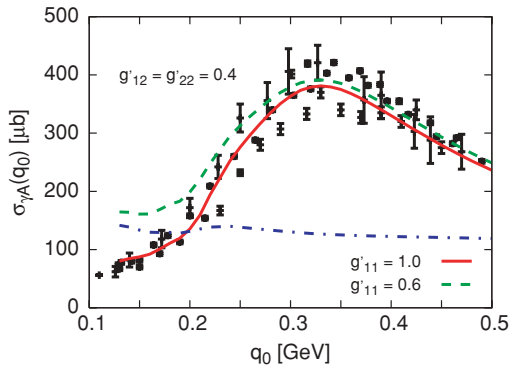

FIG. 5. (Color online) Photoabsorption cross section for $g'_{11} = 1.0$ (solid line) and $g'_{11} = 0.6$ (dashed line). We use $\Sigma_S^\Delta = -0.2$ GeV and $\Sigma_V^\Delta = -0.09$ GeV. In addition we show the background contribution for the run with $g'_{11} = 0.6$ (dash dotted line). The data are taken from Ref. [2].

In Fig. 6 we study the importance of various contributions and approximations. In the left upper panel the contributions of the resonance, background, and two-particle-one-hole states are compared with the full result. The background contribution, defined by all but the first diagram of Fig. 3, is essentially flat and delivers about 100 μb to the cross section. The resonance itself contributes about 200 μb in the peak whereas the two-particle-one-hole final states deliver an additional 50 μb. As can be seen, when adding up all contributions incoherently interference effects play a minor role only. We turn to the upper right panel of Figure 6, which illustrates the importance of vertex corrections. The

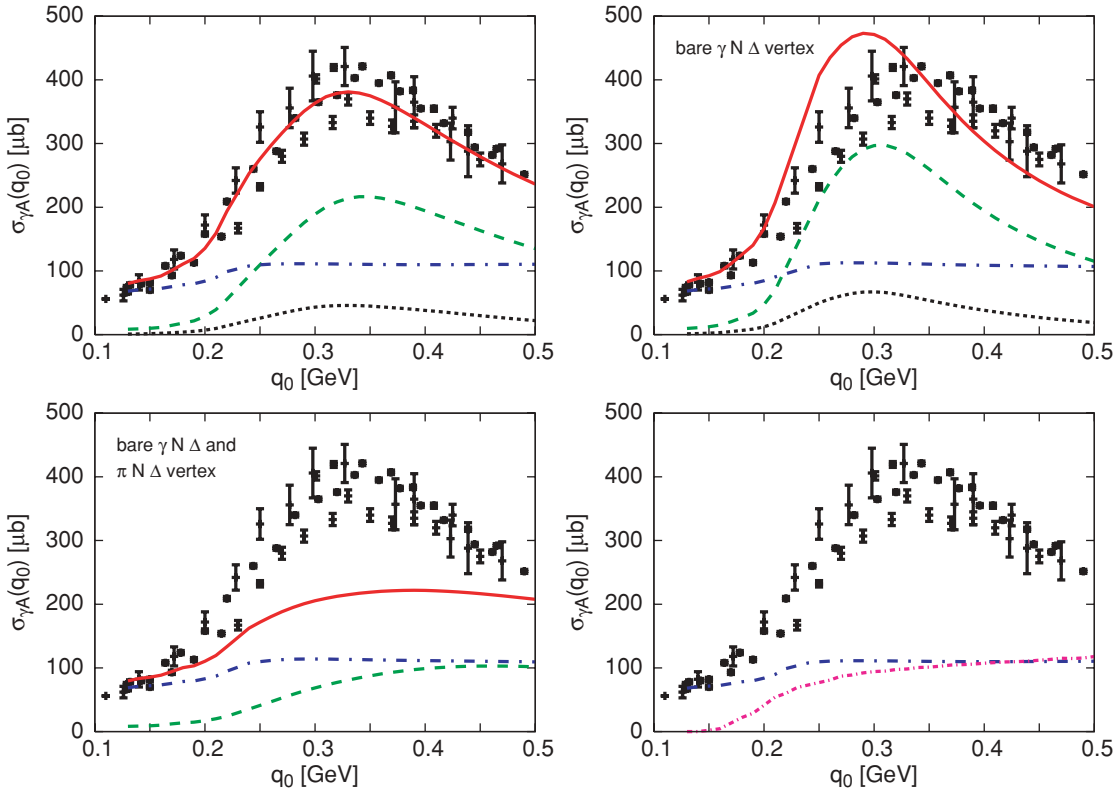

FIG. 6. (Color online) Photoabsorption cross section using the parameter set (20). The upper left panel shows the relevance of various contributions; the upper right panel shows the effect of short-range correlations in the $\gamma N\Delta$ vertex. The lower left panel follows if bare $\gamma N\Delta$ and $\pi N\Delta$ vertices are assumed. The solid lines give the complete calculations, the dashed lines the resonance contributions, the dashed-dotted lines the background contributions, and the dotted lines the two-particle-one-hole contributions. The lower right panel illustrates the importance of in-medium effects on the background processes. The short-dashed dotted line provides the background contribution evaluated with bare vertices and a free-space pion. The data are taken from Ref. [2]. See the text for more details.

solid line of that panel gives our result implied by the parameter set (20) but a bare $\gamma N\Delta$ vertex in the production amplitudes $T_{\gamma N\to\pi N}$ and $T_{\gamma N\to \mathrm{phN}}$ of Eqs. (8). The neglect of short-range correlation effects in the $\gamma N\Delta$ vertex implies a significant shift of the isobar strength about 50 MeV toward lower energies. Thus the apparent peak position seen in the absorption cross section does not directly reflect the isobar contribution. A realistic prediction of the in-medium isobar mass requires the proper consideration of such effects. An even more dramatic influence of short-range correlation effects is documented by the lower left panel of Fig. 6. Here we assume again the parameter set (20) but also bare $\gamma N\Delta$ and $\pi N\Delta$ vertices. The pion and isobar propagators used are obtained within the self-consistent and covariant approach [16], where correspondingly a bare $\pi N\Delta$ vertex was taken. This calculation corresponds to the dashed lines in Fig. 4 of Ref. [16]. As anticipated by our previous study [16] a neglect of short-range correlation effects in the $\pi N\Delta$ vertex leads to a much broader isobar, which then translates into an almost flat photoabsorption cross section. We finally turn to the lower right panel of Fig. 6. Here we focus on the background contributions. The dashed-dotted line shows the full background contribution, and the short dashed-dotted line gives the result for the background processes implied when using a bare pion propagator and bare vertices in Fig. 3. The vertex corrections in the background terms are essential to keep our approach consistent. An approximative treatment in which the in-medium spectral distribution of the pion is neglected would lead to a strong underestimation of the background processes. In this case the Pauli-blocking effect would cut away the low-energy cross section, as can be seen from Fig. 6. We emphasize that the consideration of such effects is crucial to arrive at a realistic estimate for Migdal's parameter g'_{11}.

It is interesting to compare our results with previous studies. We find a qualitative agreement with the results of Ref. [5], in which an attractive mass shift for the isobar in nuclear matter based on a perturbative and nonrelativistic many-body approach was claimed. This is in stark contrast to the more recent works using nonrelativistic vertices [10,15], in which small and repulsive mass shifts of the isobar in cold nuclear matter are claimed. As emphasized in Ref. [21] the nonrelativistic limit of Migdal's short-range correlations depends crucially on the energy of the particle-hole state. Only at zero energy do the relativistic vertices of Eq. (1) recover a conventional nonrelativistic approach. Moreover, in Refs. [10,15] important short-range correlation effects are not considered and a soft and phenomenological form factor in the $\pi N\Delta$ vertex is used. The latter reduces the effect of vertex corrections significantly. Consequently, our results will deviate from Refs. [10,15] also in the nonrelativistic limit.

Finally, the use of scalar and vector mean fields for the nucleon in our work constitutes a significant improvement over the nonrelativistic treatment thereof in Refs. [10,15]. In our case the subtle interplay of scalar and vector mean fields leads to an repulsive net energy shift as required for instance by empirical nucleon optical potentials.

IV. SUMMARY

We presented a first computation of the nuclear photoabsorption cross section that considered the effect of short-range-correlation effects in the $\gamma\,\pi\,\pi$, $\gamma\,N\,\Delta$, $\gamma\,\pi\,N\,\Delta$, $\pi\,N\,\Delta$, and $\pi\,N\,N$ vertices. We applied the self-consistent and covariant many-body approach developed by the authors for the $\pi N\Delta$ systems in the presence of short-range correlation effects. In particular the in-medium interference of the s-channel isobar exchange and the t-channel pion exchange was evaluated consistently with an in-medium pion propagator. It was shown that the latter plays an important role in the determination of Migdal's parameter $g'_{11} \simeq 1.0$, for which we obtained a rather large value. An accurate reproduction of the photoabsorption data was achieved. Based on our analysis we predict an attractive mass shift of about 50 MeV for the isobar in cold and saturated nuclear matter.

Our results ask for further detailed studies to further scrutinize the possibility of an unconventionally large g'_{11} parameter. The evaluation of crossed diagrams in the photoabsorption cross section and their possible destructive interference effects with the diagrams considered in our work should be pursued. Also the influence of the ρ meson on Migdal's short-range correlation effects as it emerges in our self-consistent and covariant many-body approach is an important topic of future work.

ACKNOWLEDGMENTS

F.R. acknowledges useful discussions with J. Knoll and would like to thank the FIAS (Frankfurt) for support. C.L.K. would like to acknowledge financial support by the Hungarian Research Foundation (OTKA Grant No. 71989) and to thank the G.S.I. (Darmstadt) and the K.V.I. (Groningen) for their kind hospitality.

[1] M. Hirata, J. H. Koch, F. Lenz, and E. J. Moniz, Ann. Phys. (New York) **120**, 205 (1979).
[2] J. Ahrens *et al.*, Phys. Lett. **B146**, 303 (1984); N. Bianchi *et al.*, *ibid.* **B299**, 219 (1993); Th. Frommhold *et al.*, Z. Phys. A **350**, 249 (1994); N. Bianchi *et al.*, Phys. Rev. C **54**, 1688 (1996).
[3] M. Kohl *et al.*, Phys. Lett. **B530**, 67 (2002).
[4] E. Oset, H. Toki, and W. Weise, Phys. Rep. **83**, 281 (1982).
[5] E. Oset and L. L. Salcedo, Nucl. Phys. **A468**, 631 (1987).
[6] R. C. Carrasco and E. Oset, Nucl. Phys. **A536**, 445 (1992).
[7] L. Xia, P. J. Siemens, and M. Soyeur, Nucl. Phys. **A578**, 493 (1994).
[8] C. L. Korpa and R. Malfliet, Phys. Rev. C **52**, 2756 (1995).
[9] P. Arve and J. Helgesson, Nucl. Phys. **A572**, 600 (1994).
[10] R. Rapp, M. Urban, M. Buballa, and J. Wambach, Phys. Lett. **B417**, 1 (1998).
[11] C. L. Korpa and M. F. M. Lutz, Nucl. Phys. **A742**, 305 (2004).
[12] M. Post, S. Leupold, and U. Mosel, Nucl. Phys. **A741**, 81 (2004).
[13] F. Riek and J. Knoll, Nucl. Phys. **A740**, 287 (2004).
[14] C. L. Korpa and A. E. L. Dieperink, Phys. Rev. C **70**, 015207 (2004).
[15] H. van Hees and R. Rapp, Phys. Lett. **B606**, 59 (2005).
[16] C. L. Korpa, M. F. M. Lutz, and F. Riek, Phys. Rev. C **80**, 024901 (2009).
[17] T. E. O. Ericson and W. Weise, *Pions and Nuclei* (Clarendon Press, Oxford, 1988).
[18] A. B. Migdal *et al.*, Phys. Rep. **192**, 179 (1990).
[19] J. Nieves, E. Oset, and C. Garcia-Recio, Nucl. Phys. **A554**, 554 (1993).
[20] M. Nakano *et al.*, Int. J. Mod. Phys. E **10**, 459 (2001).
[21] M. F. M. Lutz, Phys. Lett. **B552**, 159 (2003); **B566**, 277(E) (2003).
[22] M. MacCormick *et al.*, Phys. Rev. C **53**, 41 (1996).
[23] H. van Pee *et al.*, Eur. Phys. J. A **31**, 61 (2007).
[24] T. Fujii *et al.*, Nucl. Phys. **B120**, 395 (1977).
[25] V. Pascalutsa and D. R. Phillips, Phys. Rev. C **67**, 055202 (2003).
[26] M. F. M. Lutz and C. L. Korpa, Nucl. Phys. **A700**, 309 (2002).
[27] M. F. M. Lutz, C. L. Korpa, and M. Möller, Nucl. Phys. **A808**, 124 (2008).